MODELING AND SIMULATION OF A 100 HP PERMANENT-MAGNET BRUSHLESS DC MOTOR PROTOTYPE

WANDERLEI MARINHO DA SILVA*
IPEN-CNEN-COPESP -
Av. Prof Lineu Prestes, 2242
Cidade Universitária
CEP: 05598-900, São Paulo - Brazil

ANTONIO MELO DE OLIVEIRA
Escola de Engenharia Elétrica UFG
Goiania - Goiás - Brazil

CÍCERO COUTO DE MORAES
Depto. Energia e Automação EPUSP
Dir. Téc. Ind./Com. LAVILL -
São Paulo - Brazil

Abstract

This paper describes the mathematical modeling and related simulation results of a 100 HP electronically commutated permanent-magnet motor prototype, conceived for naval propulsion [1], based on the solution of differential equations with the SIMNON [2] software. Fürsich [4], made the first mathematical modeling for this kind of motor attempting only the armature behavior. Oliveira et al [8], showed the modeling of this prototype including armature, torque equation and operation logic. Here, a complete modeling is presented taking into account motor/load and drive operation allowing armature reaction analysis, sensor positioning, torque ripple, faults occurrence and applied voltage control. These results are compared with laboratory measurements. The interest in predicting the performance of this kind of motor has become evident in recent years, turning into a preliminary and an essential part in the motor and drive design. In order to achieve the best performance from the drive obtained, simulation is used to predict behavior and performance, to aid design and attain better understanding of the system.

Keywords

Permanent-magnet motor
Brushless DC motor
Simulation
Modeling
Marine electric propulsion
Drives

Introduction

Basic aspects of the prototype

The optimization of electromechanical energy conversion is related to the improvement of materials, efficiency, reliability, allied to simple construction and smaller weight / volume ratio, keeping the same characteristics of torque x rotation of DC motors, but without mechanical commutator inconvenients, became motive of interest for electrical machines, power electronics and control researchers. The motor and its drive that join all these characteristics, became reality with the Brushless DC Motor-BDCM [3], with multiple-phases and permanent magnets. When compared with conventional brush DC motors traditionally used for naval propulsion systems. Even compared to induction, synchronous and reluctance motors, it is more advantageous according to Fürsich [4]. The modeled and simulated prototype has similar characteristics to the drives presented by Fürsich [4], Saint Michel & Riotte [5] and Soyk [6]. The machines of these drives are permanent-magnet motors with electronic commutation for naval propulsion applications. The prototype designed and contracted by COPESP, described in previous papers [7], [8] and [9], has the basic characteristics:

Motor:

Rated power	75 kW
Rated speed	600 rpm
Number of phases	6
Number of poles	12
Rated voltage	600 V
Rated current	29 Arms per phase
Rotor's magnets	Samarium-Cobalt

Inverter:

Type	"H" bridge
Number of inverters	6
Switching device	bipolar transistor
Operating frequency	500 to 3 kHz
Modulation technique	PWM – multiple pulse width modulation
Position sensors	inductive type
Speed sensor	AC tacho generator
Current sensor	Hall effect sensor

Figures 1 and 2 show the block diagram of brushless DC motor prototype and its inverter respectively.

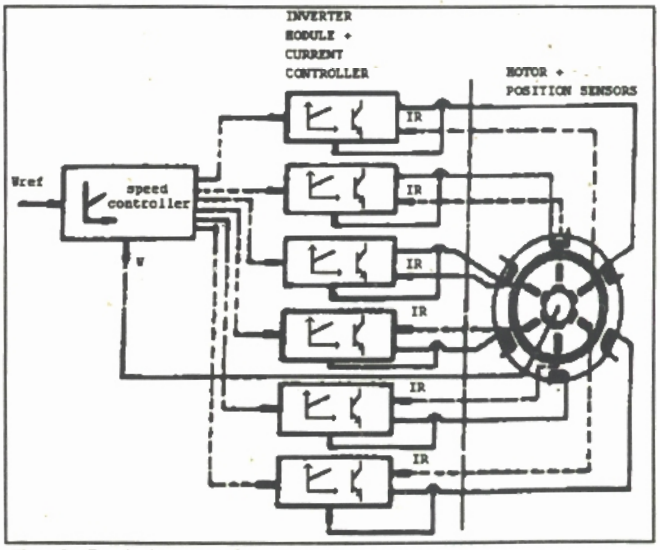

Fig. 1. Prototype scheme

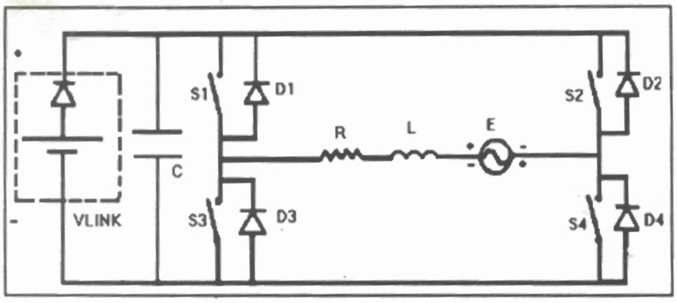

Fig. 2. "H" Inverter type.

Figure 3 shows the radial cross section rotor components.

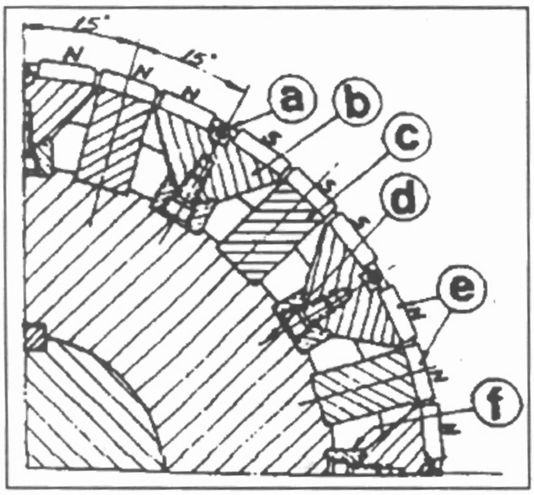

Fig. 3 Rotor: a) damping windings; b) and c) pole yokes; d) rotor pole yokes support; e) permanent-magnet and f) nonmagnetic material

Mathematical model and simulation:

Commercial software is suitable to conduct the mathematical modeling allowing, the prediction of steady-state performance, transients and faults' analysis. In this way, the consequences of inadequate sensor positioning, damage of power switches or commutation logic error, for example, may be anticipated. The mathematics models may be based either on measured or calculated parameters. The effects on the magnetic induction airgap waveform due to the magnetic poles' geometry, stator currents and slots' skewing may also be considered in this modeling.

The mathematical equations that describe the behavior of the prototype at steady-state and dynamic operation mode were simulated by the SIMNON software. The equations according to Pillay [10], were adapted to a six phase BDCM, and the simulated results compared with measurement results. The aim of this work is to validate this mathematical model, so that it can be used as a design tool for new motors and drives with different phase numbers and power. The prototype described in the introduction is modeled using state space equations:

$$\dot{\bar{x}} = A\bar{x} + B\bar{u}$$

$$\bar{y} = C\bar{x} \qquad t \geq t_o \qquad (1)$$

These equations describe a linear system, characterized by the matrices A, B and C, whose elements are constants. The mathematical model of the motor is obtained taking into account fundamental dynamic equations (2 to 9) in order to represent the machine, electromagnetic and electromechanical phenomena. The prototype modeled was divided in four parts: motor, drive, control and load.

Armature equations:

The state space equation that represents armature and its six (6) phase windings is:

$$[\dot{i}] = -[L]^{-1}[Ra][i] - [L]^{-1}[E]^T + [L]^{-1}[Va]^T \qquad (2)$$

where:

$$[i] = \begin{bmatrix} i1 \\ i2 \\ i3 \\ i4 \\ i5 \\ i6 \end{bmatrix} [Ra] = \begin{bmatrix} Ra1 & 0 & 0 & 0 & 0 & 0 \\ 0 & Ra2 & 0 & 0 & 0 & 0 \\ 0 & 0 & Ra3 & 0 & 0 & 0 \\ 0 & 0 & 0 & Ra4 & 0 & 0 \\ 0 & 0 & 0 & 0 & Ra5 & 0 \\ 0 & 0 & 0 & 0 & 0 & Ra6 \end{bmatrix}$$

$$[L] = \begin{bmatrix} L11 & M12 & M13 & M14 & M15 & M16 \\ M12 & L22 & M12 & M13 & M14 & M15 \\ M13 & M12 & L33 & M12 & M13 & M14 \\ M14 & M13 & M12 & L44 & M12 & M13 \\ M15 & M14 & M13 & M12 & L55 & M12 \\ M16 & M15 & M14 & M13 & M12 & L66 \end{bmatrix}$$

$$[V_a] = [V_{a1} \quad V_{a2} \quad V_{a3} \quad V_{a4} \quad V_{a5} \quad V_{a6}] \qquad (3)$$

$$[E] = kw[f_{(\Theta)}] \qquad (4)$$

and

$$[f(\Theta)] = [f1 \quad f2 \quad f3 \quad f4 \quad f5 \quad f6] \qquad (5)$$

k: motor project constant
$f_{(\Theta)}$: normalized magnetic induction waveform in the airgap
θ: mechanical angle
w: angular frequency of rotor
Rii: stator resistance
Lii: self inductance
Mij: mutual inductance
E: induced voltage
Va: armature applied voltage

Mechanical equation: The mechanical equation considered to model the motor is:

$$Tm(t) - TL(t) = J\frac{dw}{dt} \qquad (6)$$

where:

$$Tm = k\left[f_{(\Theta)}\right][i] \qquad (7)$$

and

$$TL(t) = Bp.w^3 \qquad (8)$$

then

$$\dot{w}(t) = \frac{Tm(t)}{J} - \frac{TL(t)}{J} \qquad (9)$$

where:

J: (motor + load) inertia
Bp: propeller dynamic friction coefficient
Tm: electromagnetic torque
TL: load torque

The $f_{(\Theta)}$ function used in equation (7) takes into account the effects on the magnetic induction waveform referred. This function is obtained either from finite element method (FEM) or tests results. P.P. de Paula [9] showed from static torque results that the prototype has negligible armature reaction and this fact is taken into account in our simulation.
To perform the $f_{(\Theta)}$ function, one cycle of the induced phase voltage at stator terminal is measured with the prototype operating as a generator without load. This induced phase voltage is a "mirror" of the magnetic induction waveform in the airgap. This waveform is then normalized, placed in a look-up table f(Θ) and used for SIMNON program.
This information allows the selection of the best drive and control strategy aiming the optimization of the armature currents waveforms. This control strategy leads to an improvement on performance due to the increase of the average torque and decrease in torque ripple, besides the reduction in the current ripple.

Validation and results:

The simulation was compared with measured results from a 100 HP prototype, aiming the mathematical model validation as a design tool to other similar motors. The mathematical model allows the evaluation of each parameter acting individually on the drive performance. This fact shows the importance of simulation, because this evaluation would be very difficult in a test, since the electromagnetic and electromechanical conversion phenomena occur simultaneously.

Figure 4 shows simulated induced and applied voltage and figure 5 shows measured voltage and current.

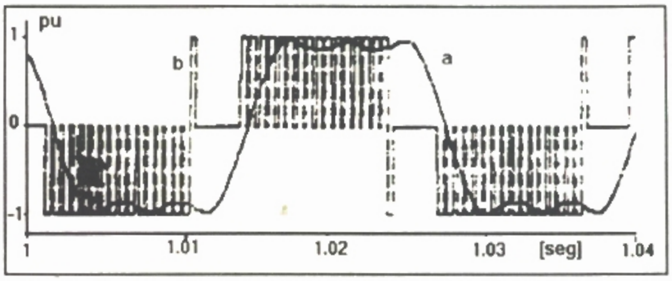

Fig. 4 Simulated (in pu) a) induced voltage and b) applied voltage.

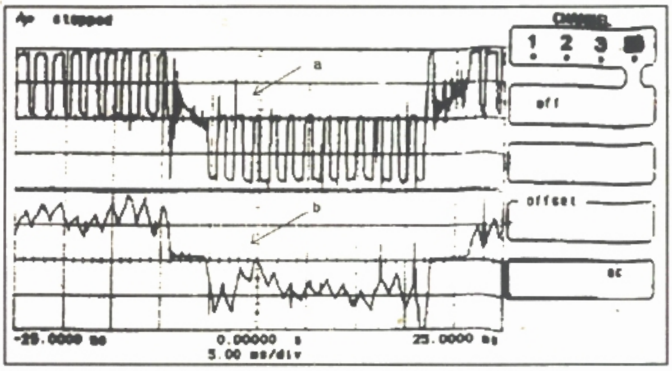

Fig. 5 Measured a) applied voltage (150 V/div) and b) current (10 A/div), PWM frequency = 1000 Hz, Vlink=300V, 300 rpm

Figure 6 shows measured phase current, and in figure 7 simulated current for TL=1200 Nm.

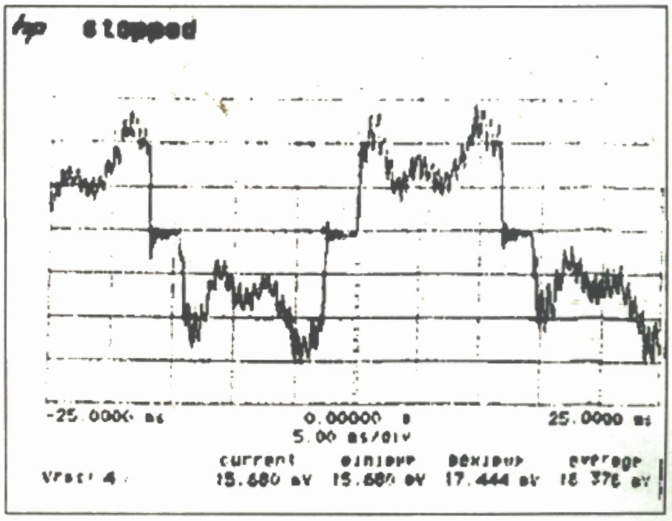

Fig. 6 Measured phase current (10 A/ Div.) for: Vlink=600 V, sensor advance 30°, PWM frequency=1670 Hz

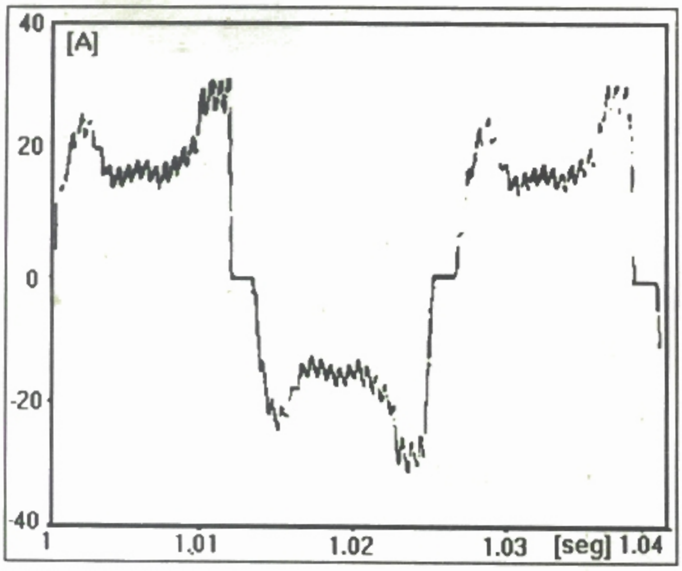

Fig. 7 Phase current Simulated for: Vlink=600 V, sensor advance 30°, PWM frequency=1670 Hz

The armature current and speed controllers showed in figure 1 were designed using conventional DC motor optimization technique (magnitude and symmetric optimum criterion of linear control system) [1], [11 and [12]. This choice is due to the fact that these prototype performance equations and that of a DC motor with constant field current are the same. The motor was simulated in closed-loop mode using these controllers and the results are showed in figure 8.

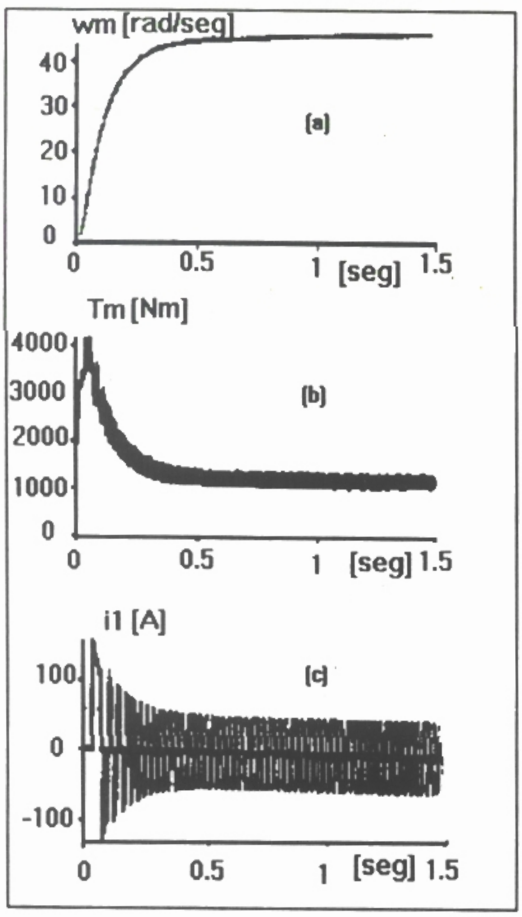

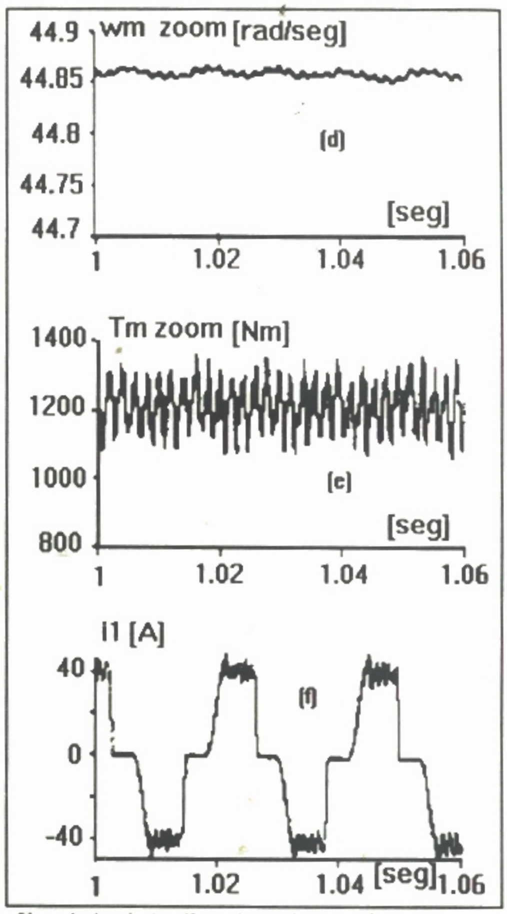

Fig. 8. Simulated starting transient: a) motor speed; b) Electromagnetic torque; c) Current phase Simulated steady-state: d) motor speed, e) Electromagnetic torque; f) Current phase were d), e) and f) are a), b) and c) waveforms in zoom mode

Figure 9 and 10 show the simulated open and closed-loop speed change curves respectively, due step loads of 20% and 40% of rated torque.

Figure 11 shows the simulated speed response for open and closed-loop operation where the overshoot response attenuation due reference signal input filter of the speed controller and system velocity are compared.

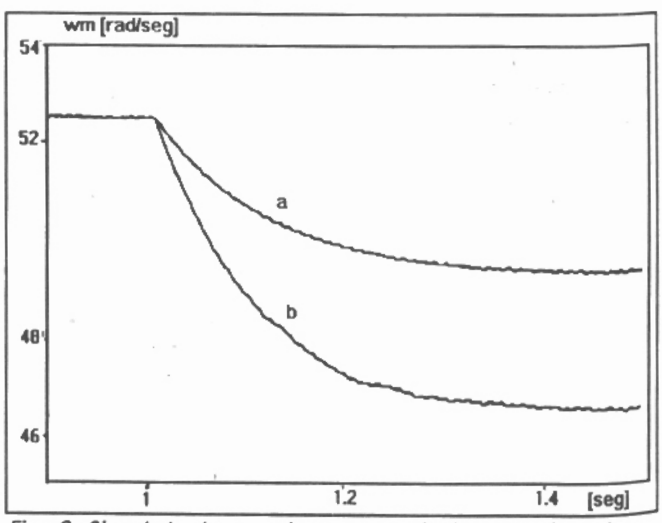

Fig. 9. Simulated open-loop speed change due step loads of a) 20% and b) 40% of rated torque

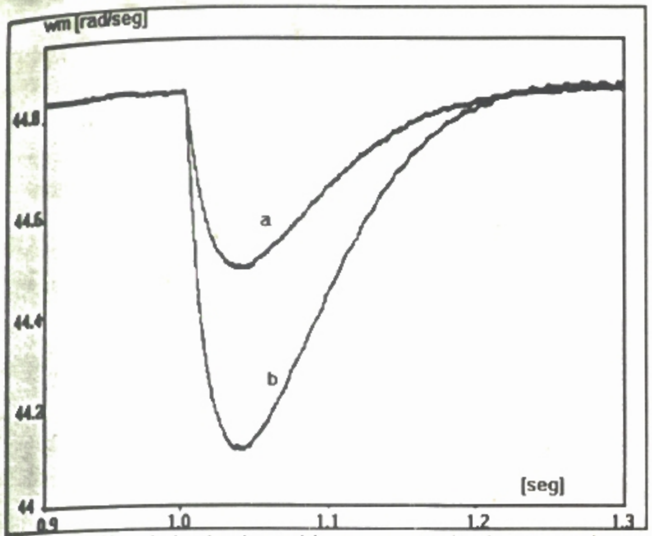

Fig. 10. Simulated closed-loop speed change due step loads of a) 20% and b) 40% of rated torque

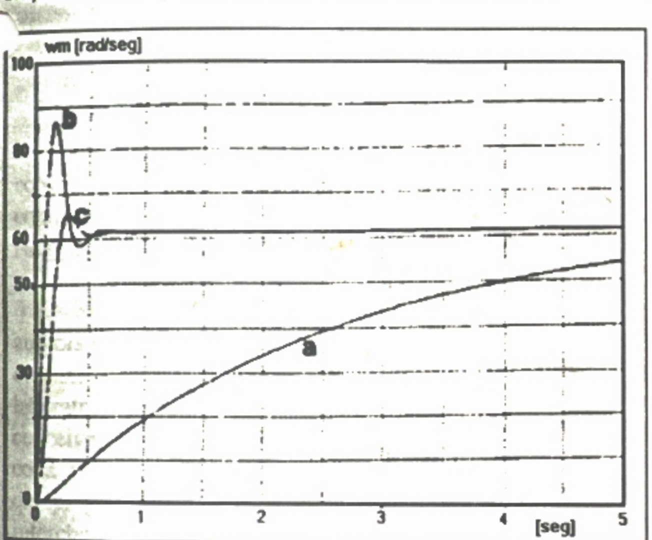

Fig.11 Simulated speed system response curves for 100% step signal reference with: a) open-loop; b) closed-loop without input filter and c) closed-loop with input filter at speed controller reference.

Conclusions:

This paper has presented a straightforward method of modeling and simulating the steady-state and dynamic behavior of a 100 HP permanent-magnet BDCM prototype. Quite good results were obtained in open-loop mode compared with measured results on the prototype. Tests in closed-loop mode were not made yet, but we hope as good results because simulations were qualitatively identical to obtained in [4]. As a result of the comparisons, it appears that the method of analysis presented in the paper is suitable to predict instantaneous line currents, electromagnetic torque of the motor and other, for typical operation points. A 486 Personal Computer system was used to conduct simulations developments. Discrepancies in the measured and simulated are mainly due to fluctuations in DC link voltage, non ideal motor parameters, such as winding resistance and small variable winding inductance (10 %), and unbalance between phases. This modeling adopted considering tests' results, allows analysis and synthesis of increased scale propulsion motors. In fact, greater BDCM motors can be constructed with some geometric form changes (example: axial motors) and switching devices (IGBT's - Insulated Gate Bipolar Transistor) compared to this unit [13,14]. For performance prediction, the system (motor and load, static converter and controllers) may be then simulated using a commercial software.

Acknowledgments

The authors thank P. P. de Paula for his contribution and discussions about this paper, and all our colleagues at COPESP who have participated in the development of the 100 HP prototype.

References:

[1] A. M. de Oliveira. Técnicas de modelação e controle de motores de imãs permanentes para propulsão naval. Tese de doutorado - Escola Politécnica da Universidade de São Paulo, São Paulo, 1993

[2] SIMNON, User guide for MS-DOS computers, version 3.2. - Department of Automatic Control of Institute of Technology of Lund - Sweden.

[3] T. J. E. Miller. Brushless Permanent Magnet and Reluctance Motor Drives. Oxford Science Publications, New York, 1993 (second edition).

[4] H. Fürsich; E. Thun; J Hamann & D Köllensperger. New converter fed permanent-field motor. In: International Conference on Electrical Machines - ICEM'86, München, 1986.

[5] J. Saint Michel & J. P. Riotte. Propulsion by electronic motor. In: European Conference on Power electronics - EPE'89, 1989

[6] K. H. Soyk.. PM excitation motor for submarine propulsion. (without references of edition).

[7] A. M de Oliveira; A. H. Kumakura & P.P. de Paula. Protótipo de 100 CV de um motor "brushless DC motor" para propulsão naval: experimentos. In: COBEP'91, Florianópolis - SC, Brazil, December 1991.

[8] A.M. de Oliveira; A.G. Badan Palhares; A. H. Kumakura; G. Winnischofer & A. Hoshino. Analysis of a Brushless DC motor performance when faults occurrence. In. 4th European Conference on Power Electronics - EPE'91. Firenze, 1991

[9] P. P. de Paula & A. M. de Oliveira. Static torque/rotor position characteristic of a 100 HP PM brushless DC motor prototype: results of tests. In. ICEM'94, Paris , France 1994.

[10] P. Pillay & Krishnan. Modeling, simulation, and analysis of permanent magnetic motor drives, part II: the brushless DC motor drive. In. IEEE transactions on industry applications, Vol. 25, n° 2. March/April, 1989.

[11] Unland, J.W. et al; Magnitude and Symmetric optimum criterion for the design of linear control systems: what is it and how does it compare with the others?. IEEE Trans. on Ind. Appl. 26 n° 3. May/June 1990, p. 489-97

[12] Krishnan, T. et al; "Fast response DC motor speed control system. IEEE Trans. on Ind. VOl. IA-10, n° 5. Sep/Oct 1974. p. 643-51.

[13] Thomas B. Bade; Advanced electric propulsion power generation and power distribution. Naval Eng. Journal, USA March 1994.

[14] Smith R. O et al; Overview of US Navy electric propulsion technology. ICEM'94, Paris, France, p. 483-87.